JOINT INSTITUTE FOR NUCLEAR RESEARCH
Veksler and Baldin laboratory of High Energy Physics

Final Report on the START program

Reach Time Determination for level-0 triggers in MPD experiment.

Supervisor
Dr. Oleg Rogachevsky
Student
Irving Ivan Gaspar,
Mexico.
Universidad Autonoma Metropolitana

Winter session. March 3th - April 27th, Dubna 2024

Abstract

To achieve the goals of the Multi-Purpose Detector, we require an efficient trigger detector designed to provide fast and effective start pulse for Time-Of-Flight detector, with excellent time resolution. Two such detectors, the Fast Forward Detector (FFD) and mini Beam-Beam detector (miniBeBe), are currently under development. To determine their performance in various scenarios, we conducted Monte Carlo simulations to determine the reach time of the detectors. We analysed high multiplicities with $Xe + Xe$ collisions at $\sqrt{s_{NN}}$ =9.2 GeV employing PHSD and UrQMD event generators. Additionally, we considered low event multiplicities through $p + p$ collisions at $\sqrt{s_{NN}}$ =9.2 GeV using PHSD event generator. The analysis revealed that the FFD provided a superior minimum reach time respect to miniBeBe detector. Conversely, the miniBeBe detector demonstrated the lowest mean reach time for both high and low event multiplicities. Furthermore, we found some inconsistencies in the expected functioning of the FFD and Electromagnetic Calorimeter (EMcal).

Acknowledges

I would like to express my sincere gratitude to Dr. Oleg Rogachevsky, Software development Project Chief at the Veksler and Baldin Laboratoy of High Energy Physics at Joint Institute for Nuclear Research, for the opportunity to collaborate on this exciting and enriching project. Dr. Rogachevsky's assistance and support throughout my tendure in the START program (winter session 2024) were invaluable, and his expertise in software development for the MPD experiment provided important contributions to my professional growth, learning, and networking experiences.

I am deeply thankful to Dr. Ivonne Maldonado, currently working at the Veksler and Baldin Laboratoy of High Energy Physics at Joint Institute for Nuclear Research, for her unwavering support and guidance during my stay in the program. Dr. Maldonado's expertise in data analysis and our constant discussions have had a huge impact in my professional growth, and expanded my understanding of various scientific fields.

I would like to extend my heartfelt gratitude to Dr. Valyo Velichkov, Senior laboratory Assistant at the Joint Institute for Nuclear Research, Department No. 3 Hadron Physic. His mentoring and enlightening discussions on the Fast Forward Detector have shed light in my understanding of the subject matter. His mentorship and networking skills have played a pivotal role in my professional career and have had a profound impact on other aspects of my life.

Additionally, I wish to express my gratitude to D. Ilnur Ramilevich Gabdrakhmanov, Dr. Maribel Herrera, Ms. Anya Zubova, Ms. Sancia Morris, Mr. Santiago Bernal, and Ms. Oris Suárez, for warming welcoming me and making my experience during my stay enriching in every way. Their tireless support, mentoring, and professional experience has opened doors and horizons, which undoubtedly contribute to my professional and personal growth.

Lastly, I would like to express my profound and sincere gratitude to my family and friends for their tired-less support, encouragement, and effort that have made it possible for me to embark on this amusing journey. Without their love and support, none of this would have been possible.

Contents

1 Introduction

1.1 The Multi-Purpose Detector experiment at NICA

The Multi-Purpose Detector, or MPD for short, is one of the several heavy-ion collision experiments carried out at the NICA (Nucleotron-based Ion Collider fAcility) at the Joint Institute for Nuclear Research in Dubna, Russia. A schematic representation of the NICA complex is depicted in Figure 1. The main purpose of the Multi-Purpose detector is to search for new phenomena in the baryon-rich region of the quantum chromodynamics (QCD) phase diagram. The range of energy which is pretended to cover is 4 GeV $\leq \sqrt{S_{NN}} \leq$ 11 GeV by colliding several species ranging from protons to gold ions. This accelerator is also expected to work with a luminosity of up to $L = 10^{27} cm^{-2} s^{-1}$, in the specific case of gold ions.

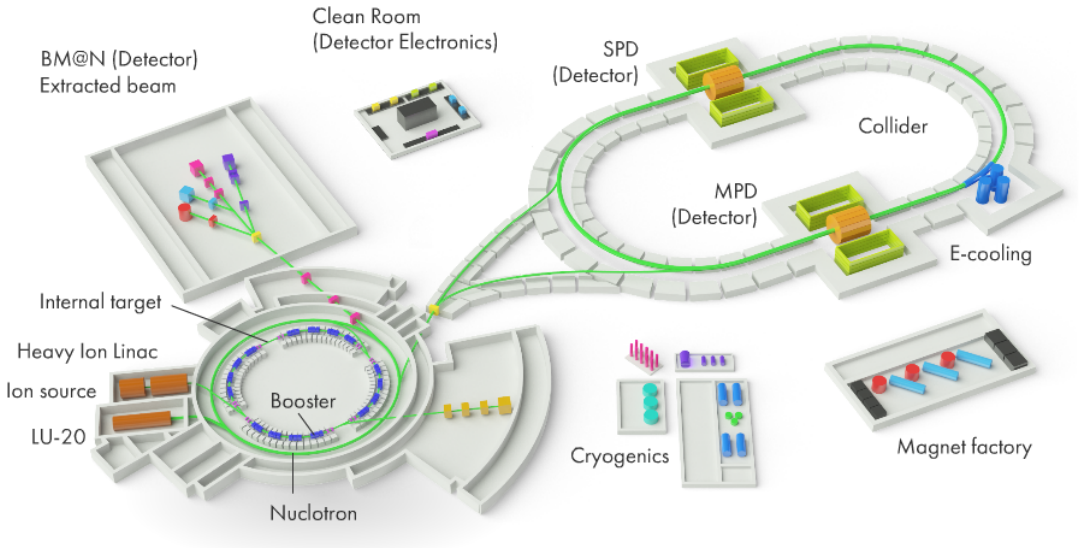

Figure 1: An overlook of the NICA complex with their main experiments, image taken for https://nica.jinr.ru/complex.php

One the major physics goals motivating the construction of the MPD is the measurement of the fluctuations and correlation patterns in the vicinity of the QCD Critical End Point. A wide variety of measurements have been performed by other experiments around the world [1–6] at higher energies. For the NICA goals, an apparatus with a solid angle coverage close to 4π and excellent particle identification capabilities at lower energies is required to obtain interesting insight into such phenomena, and the MPD will fill that gap. Furthermore, the performance of anisotropic flow measurements,comparing models studied at NICA [7–11] to the existing data [12–16] for the elliptic flow v_2 as a function of centrality, rapidity, and p_T for different species as well as higher order v_n, may indicate that a transition occurs from partonic to hadronic matter in the NICA energy range. As a consequence, it is expected that MPD provide important information on this phenomena at this energy domain. A complete description of all the physics objectives of the MPD experiment can be found in [17]. In order to achieve these physics goals the MPD has

been designed as a 4π spectrometer with the capability of detect charged hadrons, electrons and photons in heavy ion collisions, covering the energy range of the NICA collider. The MPD includes a precise 3-D tracking system and a high-performance particle identification system based on time-of-flight measurements and calorimetry detectors. A layout of the MPD apparatus is shown in Figure 2a, the setup consist mainly of the central barrel with a coverage of $|\eta| < 1.5$. The following sections are dedicated to give a description of the main components of the MPD, see Figure 2b and its particle identification capabilities.

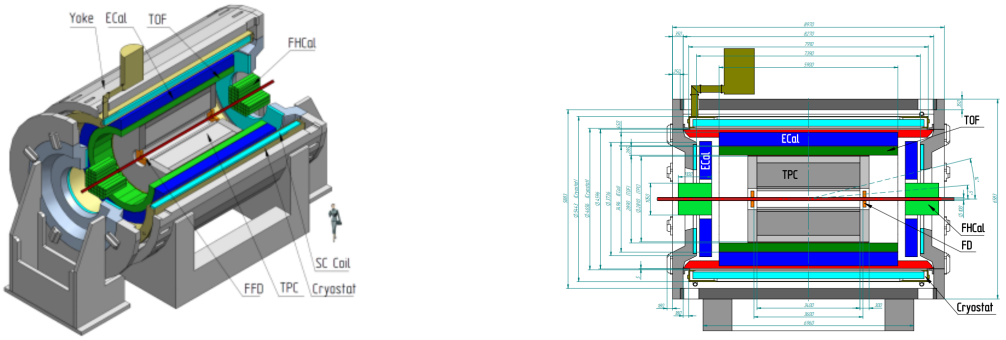

(a) MPD layout

(b) MPD subsystems, cross section in the vertical plane

Figure 2: In Figure 2a we depict the MPD central barrel. In Figure 2b we show a cross sectional view of the Central Detector by the vertical plane

1.1.1 Fast Forward Detector

The Fast Forward Detector, of FFD for short, plays an important role in the study of Au+Au collisions within the NICA energy range. The purpose of this detector is to deliver a fast and effective triggering for this collisions in the interaction point, which is intended to take place in the centre of the MPD setup. Additionally, the FFD is important for generating the start pulse for the Time-Of-Flight detector with a time resolution better than 50 picoseconds. FFD detector consists of two identical Cherenkov detector arrays, with 20 modules per side. FFD is located at ± 140 cm from the interaction point, in order to not interfere with the space dedicated to the Inner Tracking System. Additionally, they cover an acceptance of $2 < |\eta| < 4.1$ in total, see Figure 3. The Fast Forward detector detects high energy photons from the $\pi^0 \rightarrow \gamma + \gamma$ decays, charged particles, and low fragment spectators form the Au+Au collisions. The gammas are effectively detected by their conversion into electrons due to the interaction with the lead plate of thickness of 10 mm. After the electron is created, it travels through the quartz radiator, generating Cherenkov light, which is collected on a photo-cathode, perfect for obtaining great time resolution responses. Cherenkov detectors like Fast Forward Detector were also implemented in other experiments, such as PHENIX/RHIC, ALICE/LHC, and PHOBOS/RHIC, but FFD distinguishes itself by having the largest active area. Technical features and results from Monte Carlo simulations and experimental data are found in the Technical Design Report [18]. The current status of the FFD up to

the day that this report is written is depicted in the table at Figure 4, this table was presented in the XIII Collaboration Meeting of the MPD Experiment at the NICA Facility.

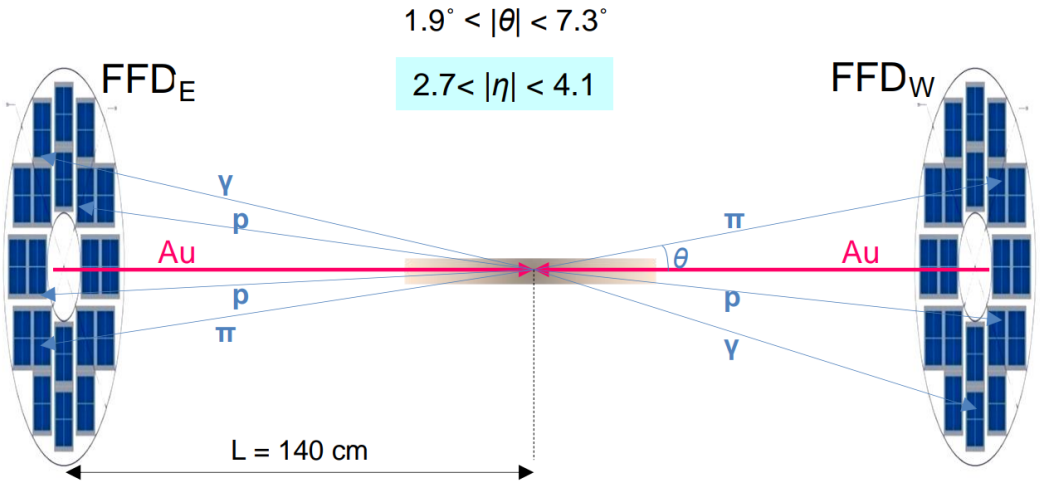

Figure 3: Representation of FFD arrays in West and East sides.

Summary

Subsystem	Readiness	Comment	Expected delay
Sub-detectors	100%	–	
Electronics	75%	Delay with production of SPM & Vertex modules	~a few months
HV & LV systems	100%	–	
Laser system	100%	–	
Cooling system	100%*	–	
DCS & Interface	80%	In progress	~6 months
Cable system	100%	–	
Long term test with cosmic rays & laser	In beginning	In progress	Tests till Dec. 2024

** A source of compressed air flow is required*

Figure 4: Status of Fast Forward Detector presented in the XIII Collaboration Meeting of the MPD Experiment at the NICA Facility, April 2024.

1.1.2 The miniBeBe detector

The miniBeBe, an acronym of "Mini Beam-Beam" counter, is a detector designed to provide a wake-up trigger signal (Level-0 trigger) for Time-Of-Flight (TOF) detector, as well as the Fast Forward (FFD) detector. To improve the trigger response, miniBeBe must efficiently handle events with low, medium and high multiplicities, such as p+p, p+A, and A+A, respectively. Despite miniBeBe sharing the goal of providing a fast trigger response with FFD detector, its main difference lies in its geometry. The miniBeBe detector consists of 8 H-shaped rails of 600 mm each in length, forming a cylindrical shape surrounding the beam pipe and covering an acceptance of $|\eta| < 1.9$, see Figure 5. These rails are made of arrays of 20 squared plastic scintillators with dimensions of 20x20x5 mm^3. In addition, each plastic EJ232 scintillators is accompanied by two Hamamatsu S13360-PE Silicon Photo-Multipliers (SiPMs) on each side of the scintillator. The radial position of each plastic scintillator has faced several changes in order to obtain better results; the original position was 22.3 cm, but nowadays, the radial position is 8.5 cm from the beam pipe. Further description concerning all the Front-End electronics and simulations for $p + p@\sqrt{s_{NN}} = 9$ GeV and $Bi + Bi@\sqrt{s_{NN}} = 9$ GeV using UrQMD event generator, carried out to probe its trigger efficiency with the previous geometry ($r = 10.0$ cm) can be found in [19]. On the other hand, the results for the new radial position of the plastic scintillators were carried out with 5M events of $p + p$ collisions, 1M events of $Bi + Bi$ collisions, and 200K events of $Xe + Xe$ collisions, all at $\sqrt{s_{NN}} = 9.2$ GeV with PHSD event generator. The current status up to the day this report is written was presented by Dr. Ivonne Maldonado at the XIII Collaboration Meeting of the MPD Experiment at the NICA Facillity in April 2024 [20]. The status of the development process and future prospects are depicted in the following timeline Figure 6.

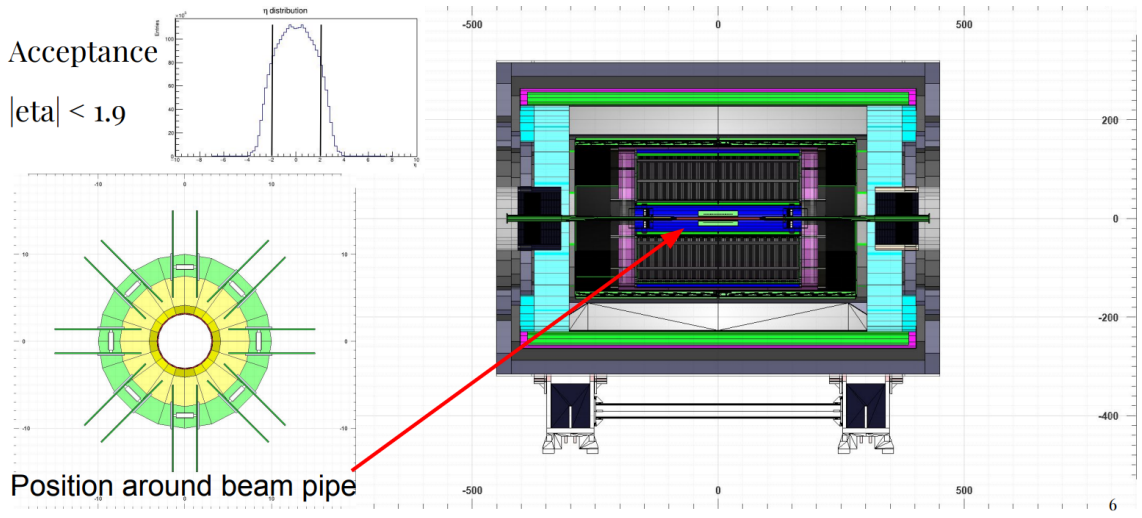

Figure 5: (Right) Representation of the location of the miniBeBe detector inside the MPD setup. (Left Bottom) Top view of the 8 H-shaped rails including the sensible parts. (Left top) Acceptance of the miniBeBe detector.

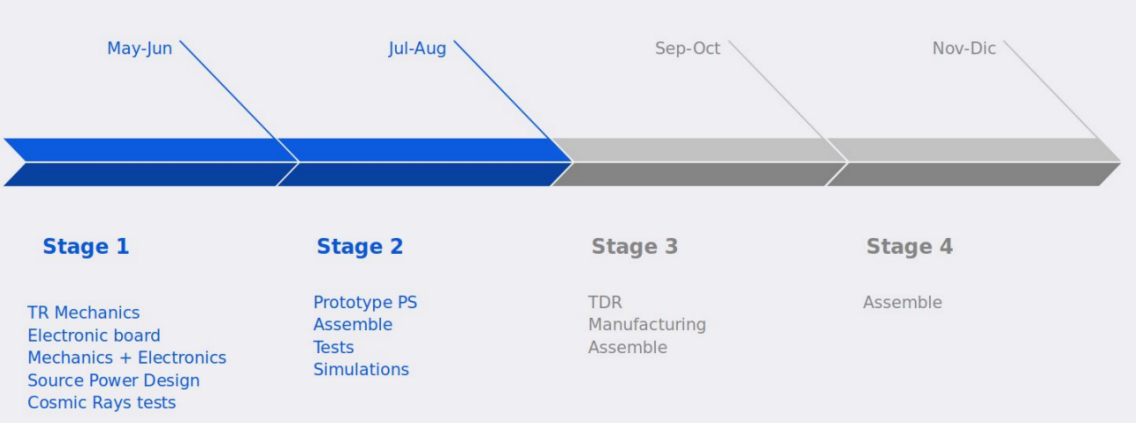

Figure 6: Timeline for the development process of the miniBeBe detector.

1.1.3 Forward Hadron Calorimeter

The Forward Hadron Calorimeter, or FHCal for short is designed for measuring the energy of nucleons or fragments that do not participate in the collision (commonly refereed as spectators), approximately with an energy of 1 GeV to 6 GeV. FHCal is also intended for determination of the collision centrality and the orientation of the reaction plane, in order to study of the collective flow concerns at NICA. The FHCal is made of two arrays placed at a distance of ± 320 cm from the interaction point, due to this location the FHCal achieves an acceptance of $2.0 < |\eta| < 5$ in pseudorapidity. Each FHCal array consists of 44 modules with a transverse size of 15x15 cm^2, each module is made of 42 lead-scintillators sandwiches, and the materials of this detector are nonmagnetic. A schematic representation of each modular array is depicted in Figure 7b, where the yellow and green modules are dedicated to performance studies. Further information about the electronics, mechanics of the detector, and performance of the FHCal for centrality and event plane can be found in the Technical Design Report [21].

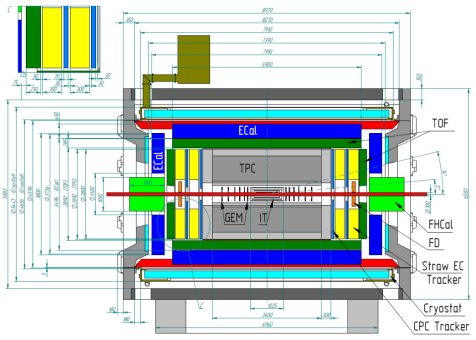

(a) Top view of the MPD set up and the FHCal subsystems in the right upper corner of the schema.

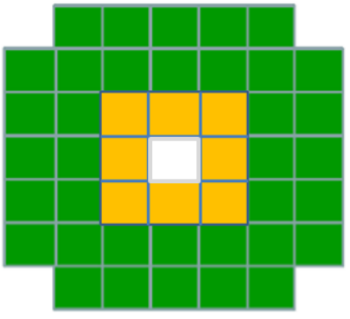

(b) Transverse view of the 44 FHCal modules with a hole in the centre for the beam pipe.

Figure 7: Schematic view for the FHCal.

1.1.4 Electromagnetic Calorimeter

The main task for the Electromagnetic Calorimeter (EMCal) is to measure, with a good resolution, the spacial position and the total deposited energy of electromagnetic cascades induced by electrons and photons as result of the collisions. Additionally, EMCal has the task to reconstruct π^0 and its momenta. The Electromagnetic Calorimeter is made of Pb-scintillator sandwiches consisting of 50 isolated half-sectors forming a cylindrical shape of 6 m long, inner radii of about 1,710 cm and outer radii of 2,278 cm. The coverage in the transverse plane for each sector is $\theta = 14.4$, see Figure 8. A half-sector contains 48 calorimeter modules, 8 modules in the longitudinal direction and 6 modules in the transversal direction.

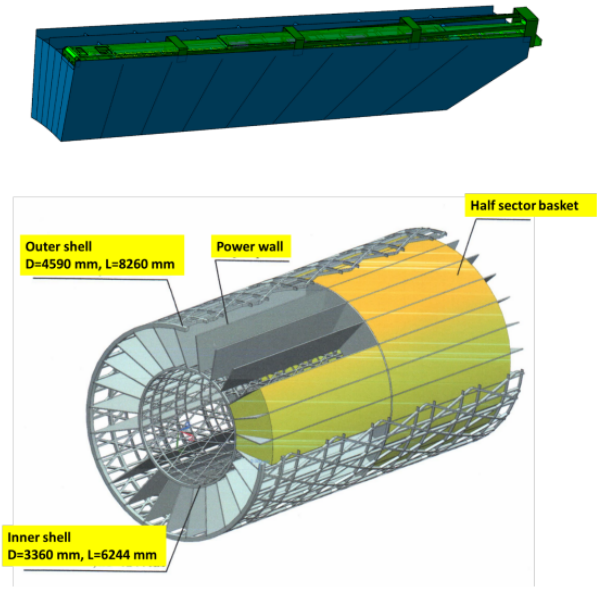

Figure 8: Schematic view for the EMCal.(Top) View of an EMCal sector. (Bottom) Structure of the EMCal inside the support frame.

1.1.5 Time Projection Chamber

The Time Projection Chamber (TPC) is designed to serve as the main tracking detector. One of the tasks for the TPC is to perform 3-D precise tracking for charged particles based on the drift time and R-ϕ cylindrical coordinate measurements of the primary ionisation clusters when the charged particles cross the detector, see Figure 9 for a schematic representation of the reconstructed tracks. Secondly, the TPC is intended to identify charged particles by measuring their specific ionisation energy loss ($\langle dE/dx \rangle$) with a resolution better than 8%. Additionally, the TPC will provide an acceptance of $|\eta| < 1.2$ and a momentum resolution for charged particles better than 3% in the range of $0.1 < p_T < 1$ GeV/c. The TPC is designed as a barrel with an inner radii of 27 cm, an outer radii of 140 cm , and 340 cm length, see Figure 10 for a schematic view of TPC. The mechanical and electronic specifications, as well as performance results are extensively described in the Technical Design Report provided by the TPC team in the LHEP at JINR [22]. The current status and the

time schedule for production and assembling to the MPD structure was presented in the XIII Collaboration Meeting of the MPD Experiment at the NICA Facility by Dr. S. Movchan, see Figure 11.

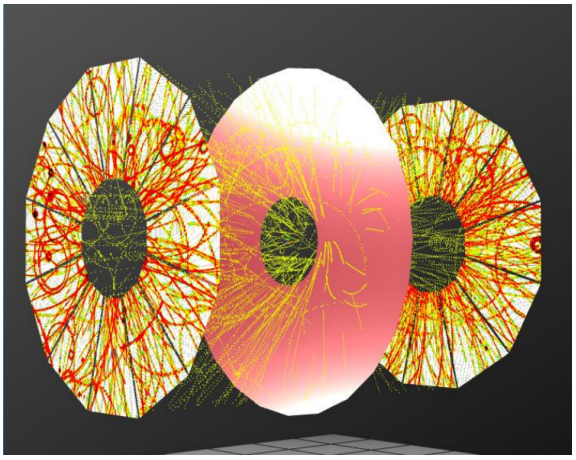

Figure 9: Schematic view of the reconstructed tracks in the TPC

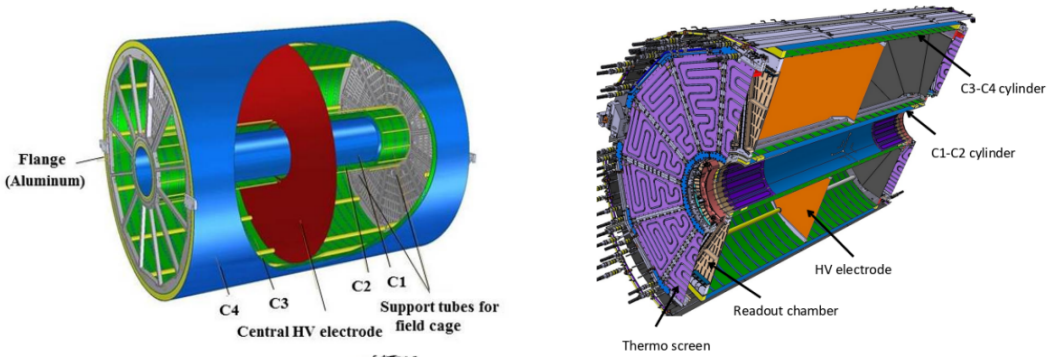

Figure 10: View of the Time Projection Chamber main components

Status:	
TPC vessel	in progress
ROCs (24+6 spare)	ready
FE electronics	81% manufactured (1217 FECs from 1500)
Gating grid system	ready
HV+LV systems	ready for start installation
Gas system	ready for start piping
Cooling system	in progress
Laser system	in progress
Slow control system	in progress
TPC assembling:	
TPC:	
TPC assembled	Dec 30 2024
TPC tests (with laser tracks and cosmic ray)	March-Sept 2024 → Jan-Feb 2025
TPC rails and installation tooling:	
Rails installation to ECAL support structure	May 30 2024
Tooling for installation TPC to MPD delivery	August 2024
TPC+ECAL cooling systems (INP BSU, Minsk):	
Delivery to JINR	Sept 30 2024
Systems assembling and tubing	Oct 27 2024
Commissioning	Nov 27 –Dec 30 2024
TPC installation to MPD	Nov 30 2024 -> March 03-May 24 2025
Cabling	Jan-June 2025
Start of MPD commissioning	from June 27 2025

Figure 11: Status and time schedule for the TPC presented in the XII Collaboration Meeting of the MPD Experiment at the NICA Facility.

1.1.6 Time of Flight

The Time Of Flight detector is designed to provide particle identification for intermediate ranges of momentum, ranging from 100 MeV/c up to 2 GeV/c. Furthermore, the TOF system must have a large phase space coverage and a good position resolution to perform effective matching of its hits with the TPC tracks. Finally, the Time of Flight must be able to separate pions and kaons with momenta of up to 1.5 GeV/c, and protons/antiprotons up to 3 GeV/c of momenta. The TOF is located between TPC and EMCal, it has a inner radii of about 1.5 m and an outer radii of 1.7 m. Following to the TOF design description, the detector is segmented respect to the transverse angle ψ into 14 pairs of modules of 5.9 m length, covering an acceptance of $|\eta| < 1.4$, see Figure 12 (left). Each module contains 10 Multigap resistive Plate Counters (mRPC) with 24 readout strips each, such material has a satisfactory timing properties and efficiency in particle fluxes. The Time Of Flight is being on construction and the current status, including a time schedule is depicted in Figure 12 (right).

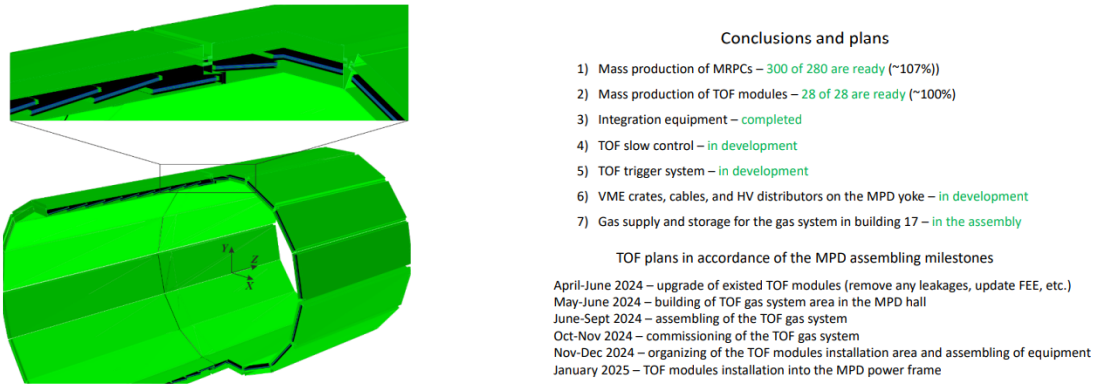

Figure 12: (Left) View of the TOF arrangements and modules, as well as a cross-section for some selected TOF modules. (Right) Brief description of the current status of the TOF presented at the XII Collaboration Meeting of the MPD Experiment.

2 Methodology

This work aims to measure the time taken by the particles involved in the collisions, as well as spectator, to be detected by each subsystem of the Multi-Purpose Detector. To include the miniBeam Beam detector, currently under development, we utilised Monte Carlo simulations. Specially, we analysed 100,000 minimum bias events for $Xe + Xe$ collisions at $\sqrt{s_{NN}} = 9.2$ GeV using the Parton Hadron String Dynamics (PHSD) event generator. Additionally, we analysed 20,000 minimum bias events for $Xe + Xe$ collisions at $\sqrt{s_{NN}} = 9.2$ GeV using Ultra relativistic Quantum Molecular Dynamics (UrQMD) model, both datasets have $\sqrt{\sigma_z} = 50$ cm.

In order to explore events with low multiplicities, we analysed 5 million of $p + p$ events using the PHSD generator, focusing on the Fast Forward Detector, Forward Hadron Calorimeter, and miniBeBe detector were considered. In order to corroborate the proper detection of species for each detector, we calculate the reach time for neutral and charged particles, including such as pions, neutrons protons, and gamma rays.

To analyse the correct behaviour of the Fast Forward Detector (FFD), we analyse 100,000 minimum bias events for $Au+Au$ collisions at $\sqrt{s_{NN}} = 5$ GeV collision using the Los Alamos Quark Gluon String Model (LAQGSM) with $\sqrt{\sigma_z} = 0$ cm. We considered both Monte Carlo simulated data and reconstructed for this particular case.

3 Results

In this study, we measure the reach time for the particles from the interaction point to each sensitive parts for each detector including the miniBeBe detector now being in production. In order to perform the analysis for the Monte Carlo data we use the MPDroot software. The performance of this task is the great importance to check the proper operation for each detector, we achieve this by depicting certain kind of species for each subsystem.

3.1 Reach time for $Xe + Xe$ collisions at $\sqrt{s_{NN}} = 9.2$ GeV

The results for Monte Carlo simulation of the reach time for Xenon-Xenon collisions using PHSD generator are depicted in Fgures 13 and 14. In Figure 13 we observe a significant number of protons and pions in all detectors across different ranges of reach time. As FFD and miniBeBe are intended to be Level 0 triggers, we will focus explicitly on their results. The first protons arriving at the FFD have a reach time of 0.118 ns, while for the miniBeBe detector, the first protons has a time of 0.151 ns. The mean reach time for the miniBeBe and FFD is 1.815 ns and 5.737 ns, respectively. For pions, we observe a minimum reach time of 0.1 ns, and 1.15 ns for FFD and miniBeBe, respectively. The mean reach time for piosn in FFD and miniBeBe is 0.671 ns and 3.614 ns, respectively. Table 1 depicts the other minimum and mean reach times for protons and pions in all the other detectors.

Detector	Min. Reach time [ns]	Mean reach time [ns]	Detector	Min. Reach time [ns]	Mean reach time [ns]
Protons			Pions		
FFD	0.188	5.737	FFD	0.1	3.614
miniBeBe	0.151	1.825	miniBeBe	0.15	0.671
FHCal	3.718	11.72	FHCal	3.918	10.74
EMCal	5.7	10.74	EMCal	5.7	7.716
TOF	5.0	10.6	TOF	5.0	7.13
TPC	1.4	6.49	TPC	1.3	2.534

Table 1: Minimum and Mean reach time for protons and pions using PHSD event generator in $Xe + Xe$ collisions.

The reach time for neutrons and gammas are depicted in Figure 14. Upon initial observation, neutrons arriving at Electromagnetic Calorimeter; however, this is an inconsistency with the detectors' function, as they identify charged particles by the interaction with matter. Furthermore, there is an absence of gammas at the FFD, which is significant considering on of the mains tasks of the FFD is to detect π^0 decay gammas.

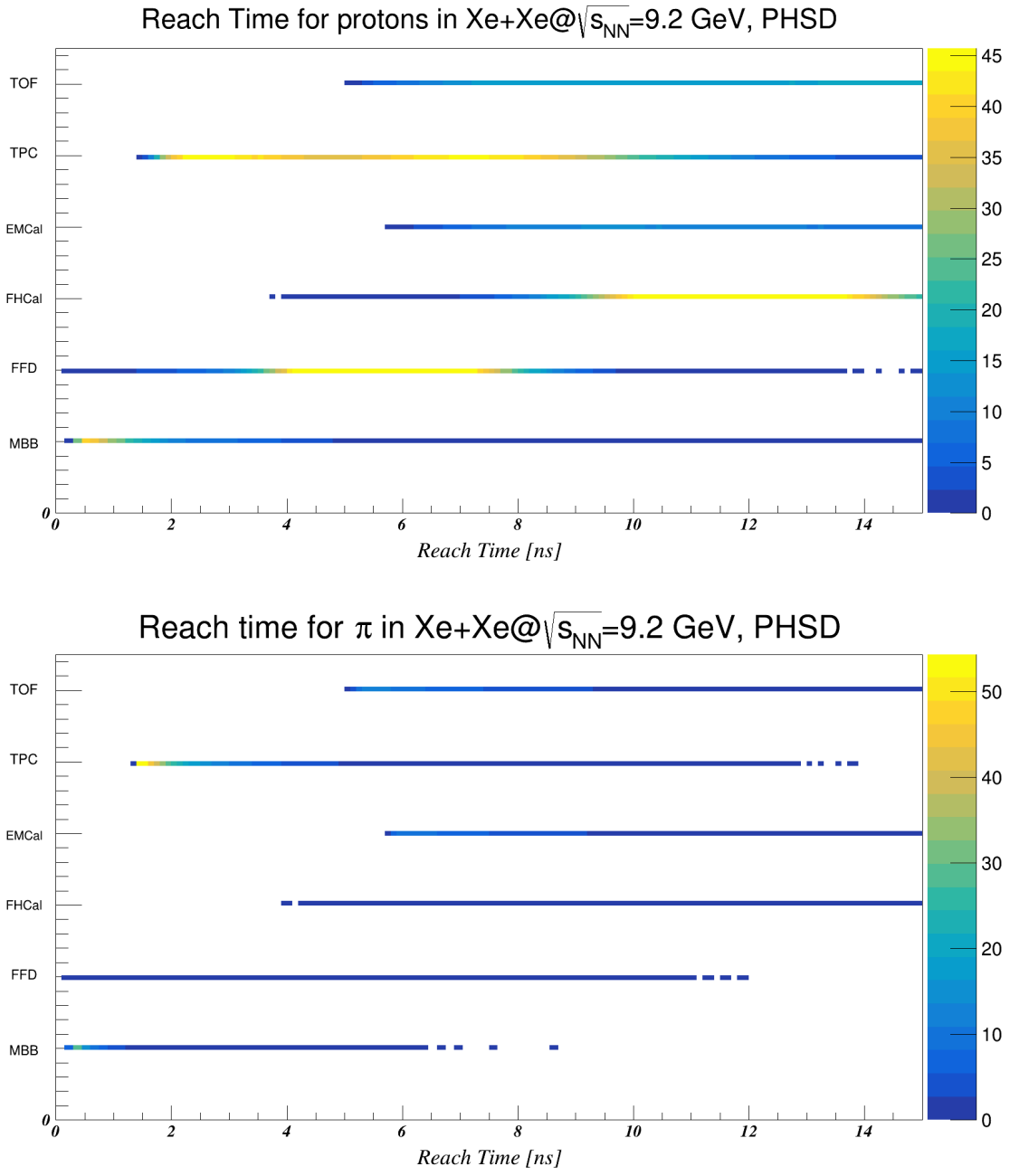

Figure 13: Reach time for protons (top) and pions (bottom) per event in $Xe + Xe$ collisions using PHSD event generator is presented. The detectors that shows minimum reach times are the Fast Forward detector (FFD) and the mini Beam-Beam detector (miniBeBe).

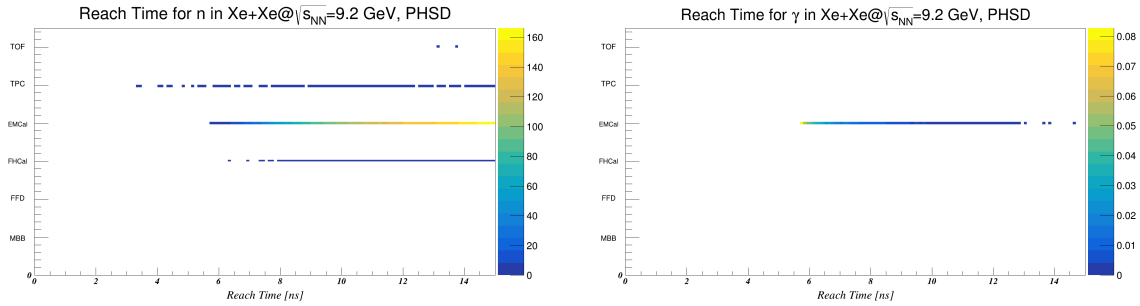

Figure 14: Reach time for neutrons (left) and gamma rays (right) per event in $Xe+Xe$ collisions using PHSD event generator is shown. Here we found inconsistencies, for example in TPC and EMCal we found neutral particles, while for FFD we do not observe gamma rays.

The results for collisions using UrQMD generator are shown in Figures 15 and 16. The reach time for protons is depicted in the Figure 15 (top), the first protons strikes the FFD material after 0.2 ns they departed from the interaction point, while the particles arrived at miniBeBe after 0.151 ns. The mean reach time for FFD and miniBeBe is 5.646 ns and 1.703 ns, respectively. In Figure 15 (bottom) we show the reach time for pions in all detectors. Here we obtain a minimum reach time of 0.1 ns and 0.15 ns for FFD and miniBebe detectors, respectively. The mean reach time for pions in FFD is 3.585 ns, while for miniBeBe is 0.645 ns. Further results for minimum and mean reach time for the remaining detectors are summarised on Table 2.

Detector	Min. Reach time [ns]	Mean reach time [ns]	Detector	Min. Reach time [ns]	Mean reach time [ns]
Protons			Pions		
FFD	0.2	5.646	FFD	0.1	3.585
miniBeBe	0.15	1.703	miniBeBe	0.15	0.645
FHCal	3.318	11.69	FHCal	3.918	10.77
EMCal	5.71	10.47	EMCal	5.7	7.759
TOF	5.0	10.29	TOF	5.0	7.337
TPC	1.4	6.112	TPC	1.3	2.511

Table 2: Minimum and Mean reach time for protons an pions using UrQMD event generator in $Xe + Xe$ collisions.

The reach time for neutrons and gammas are depicted in Figure 16. Similar to the results obtained from the collisions using PHSD generator, a significant number of neutrons is observed in the EMCal. Additionally, there is an absence of gammas, mirroring the findings from the previous analysis.

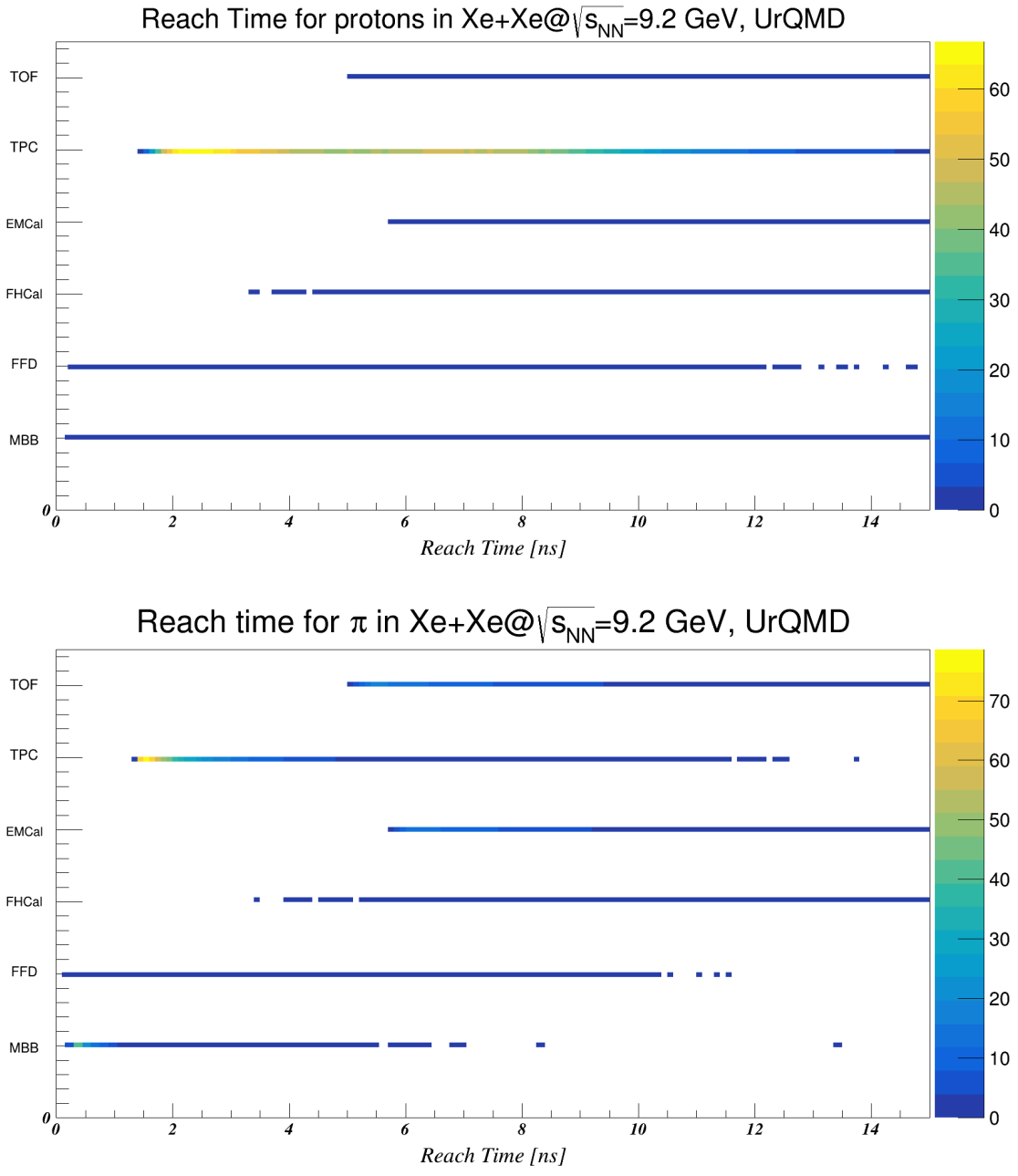

Figure 15: Reach time for protons (top) and pions (bottom) per event in $Xe + Xe$ collisions using UrQMD event generator is presented. The detectors that shows minimum reach times are the Fast Forward detector (FFD) and the mini Beam-Beam detector (miniBeBe).

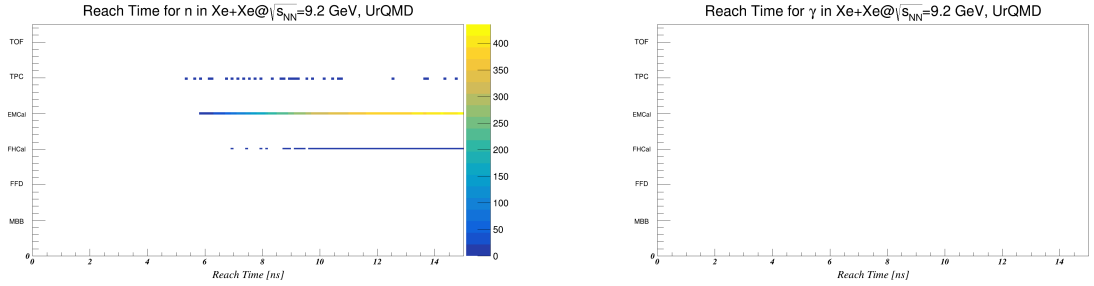

Figure 16: Reach time for neutrons (left) and gamma rays (right) per event in $Xe+Xe$ collisions using UrQMD event generator is shown. Here we found inconsistencies regarding the particle depicting, for TPC and EMCal we found neutral particles, while for FFD we do not observe gamma rays.

3.2 Reach time for $p+p$ collisions at $\sqrt{s_{NN}} = 9.2$ GeV

In order to investigate low multiplicities, Monte Carlo simulations were performed for $p+p$ collisions using PHSD event generator. The results pertaining FFD, miniBeBe and FHCal are illustrated in Figures 17 and 18. In Figure 17, the reach time for protons is depicted, the minimum values in reach time are 0.2 ns, and 0.15 ns is obtained. The mean reach time for FFD is 4.657 ns, while for miniBeBe reaches 0.15 ns. Regarding pions, the first particles reach FFD at 0.1 ns, while miniBeBe detects them at 0.15 ns. The mean reach time for FFD and miniBeBe is calculated as 3.516 ns and 0.619 ns, respectively. The minimum and mean reach time for the detectors taken into account are summarised in Table 3

Detector	Min. Reach time [ns]	Mean reach time [ns]	Detector	Min. Reach time [ns]	Mean reach time [ns]
Protons			Pions		
FFD	0.2	4.657	FFD	0.1	3.516
miniBeBe	0.15	1.53	miniBeBe	0.15	0.6196
FHCal	1.818	11.17	FHCal	2.818	10.56

Table 3: Minimum and Mean reach time for protons an pions in FFD, FHCal, and miniBebE using PHSD event generator in $p+p$ collisions.

The reach time for neutrons and gammas are presented in Figure 18. Notably, gammas are totally absent in the detectors, particularly in FFD. This raises concerns about the correct effectiveness of FFD in gamma rays identification. Furthermore, neutrons are found in FHCal, aligning with its expected functionality, as Hadron Calorimeter has the capability to detect neutral particles. This behaviour is consistent in the previous analysis.

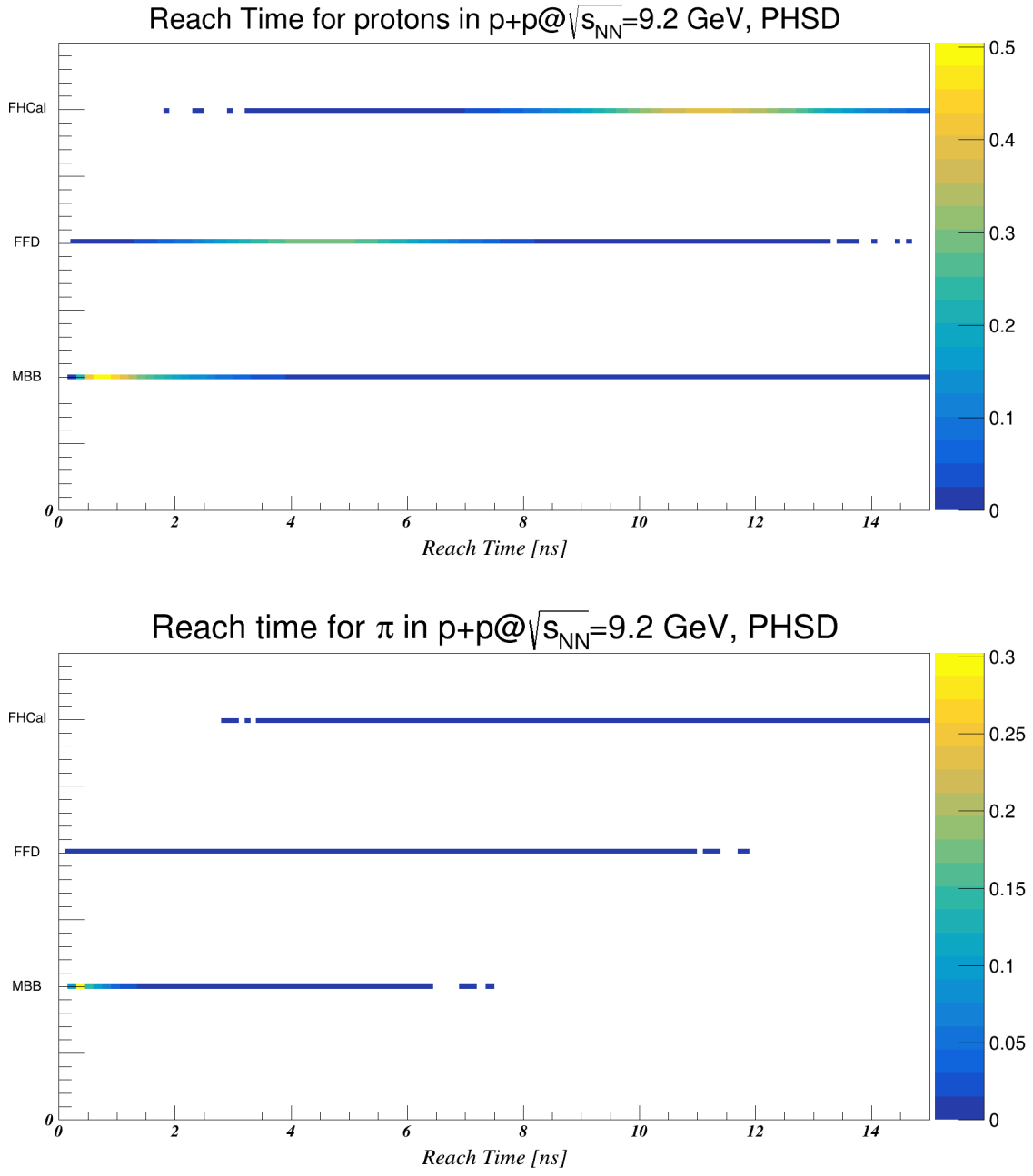

Figure 17: Reach time for protons (top) and pions (bottom) per event in $p + p$ collisions using PHSD event generator is presented. The detectors that present minimum reach times are the Fast Forward detector (FFD) and the mini Beam-Beam detector (miniBeBe).

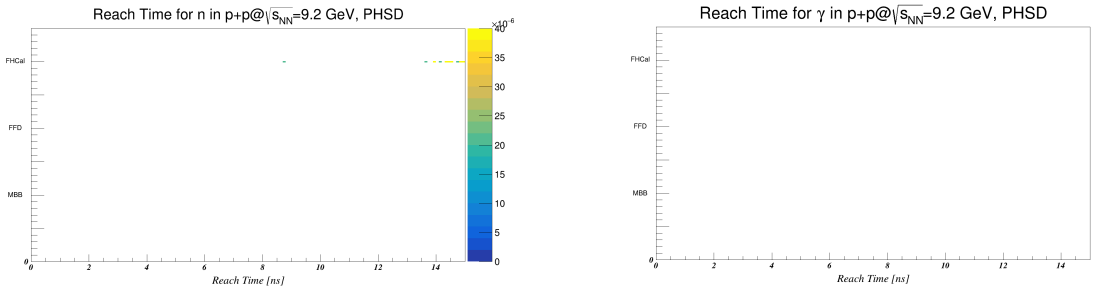

Figure 18: Reach time for neutrons (left) and gamma rays (right) per event in $p+p$ collisions using PHSD event generator is presented. Notably, gammas are totally absent in the detectors, particularly in FFD. This raises concerns about the correct effectiveness of FFD in gamma rays identification.

3.3 Fast Forward Detector gamma determination

In order to investigate the absence of gammas in Monte Carlo simulations within the Fast Forward Detector (FFD), we analysed 100,000 minimum bias events of $Au + Au$ collisions at 5 GeV. The pseudorapidity distribution of emitted gammas in neutral pion decays is illustrated in Figure 19, with the FFD pseudorapidity coverage pointed out. This histogram indicates the existence of gamma tracks that can take place in the Fast Forward Detector due to the interaction with the lead plate, generating electrons that traverse the quartz bar and produce Cherenkov photons. We implemented a cut-off energy greater than 5 MeV, corresponding to the energy threshold for pair production in the gamma-lead interaction. The energy spectra for this cut-off is shown in Figure 20, where we obtain approximately 3 gammas per event. Additionally, we analysed the points registered in FFD for electrons whose mothers are gamma rays, finding a correlation of about 3 e^-e^+ pairs per event coming from gamma rays produced in π^0 decays.

List of particles registered in FFD for Monte Carlo simulations						
Specie	p	μ	π	K	γ	e
Mult.	21	2	7	0.01	0	46

Table 4: Table of the particles detected per event by the Fast Forward Detector in the Mote Carlo simulations.

List of particles registered in FFD for reconstructed simulations								
Specie	p	μ	π	K	γ	e	n	$K^0_{L,S}$
Mult.	~ 13	$4.5x10^{-4}$	~ 4	~ 0.06	~ 2	$1.6x10^{-4}$	~ 19	~ 1.7

Table 5: Table of the particles detected per event by the Fast Forward Detector in reconstruction.

Furthermore, the particles registered in the Monte Carlo simulation for the Fast Forward detector are depicted in Table 4, those particles detected in the recon-

struction are presented in Table 5.From the latter table, we observe that of the 3 gammas identified in the Monte Carlo tracks, only 2 are detected in the data reconstruction. This discrepancy suggests us to further investigation of the accurate detection of gamma rays in the Monte Carlo simulations, represented in the software as FFDPoints, for the Fast Forward Detector in order to obtain the expected results directly.

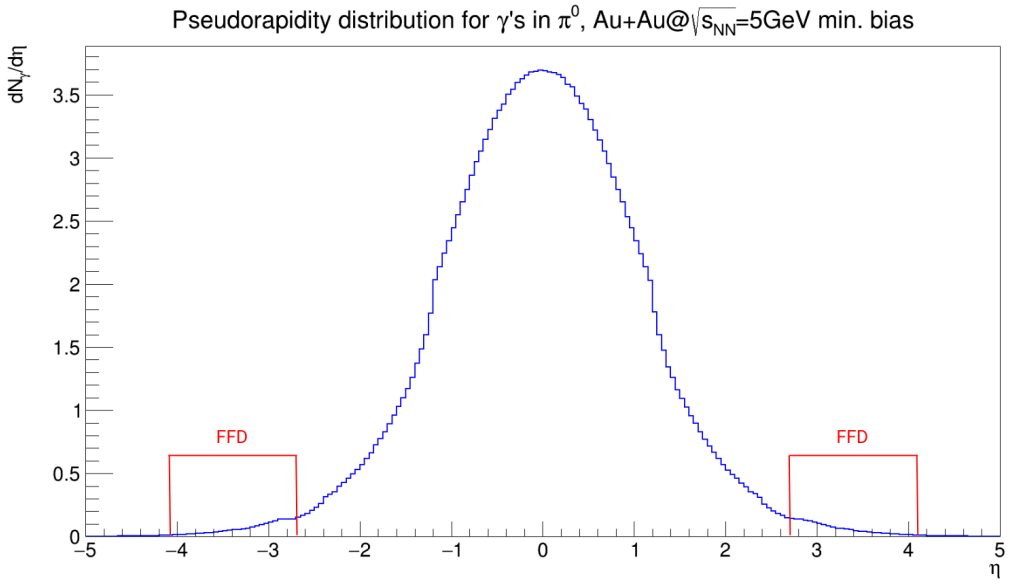

Figure 19: Pseudorapidity distribution for emitted γ from π^0 decays in $Au + Au$ collisions using LAQGSM. We can observe a no null quantity of gammas within the FFD acceptance.

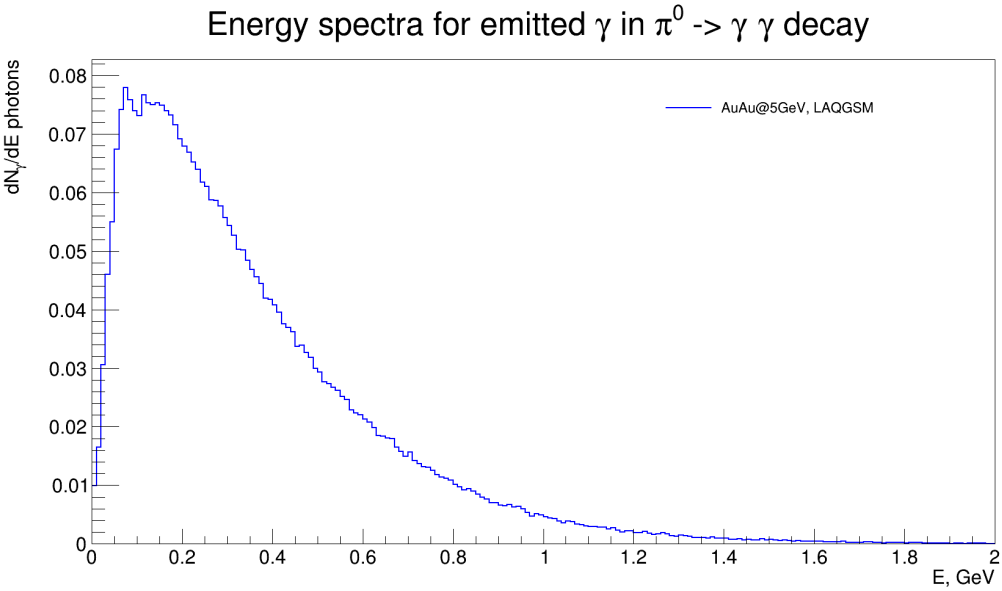

Figure 20: Energy spectra for emitted γ from π^0 decays in $Au + Au$ collisions at $\sqrt{s_{NN}} = 5$ GeV using LAQGSM. This results are similar to those found in the Technical Design Report [18].

4 Conclusions

In the study of i high multiplicities through $Xe+Xe$ collisions at $\sqrt{s_{NN}} = 9.2$ GeV, we observed important advantages of the Fast Forward Detector (FFD) in terms of reach time. FFD provided the best minimum values of reach time compared to miniBeBe, and other detectors. Notably, the minimum value for pions in FFD was registered at 0.1 ns. Conversely, the miniBeBe detector demonstrated the best mean reach time among all the detectors, with a mean recorded reach time of 0.613 ns for pions generated using the UrQMD event generator. The advantage of having a best response in minimum values of reach time lies in a good response in the start pulse for the Time-Of-Flight detector. However, as we can appreciate from the Figures 13 and 15 such rapid reach times are less frequent. On the other hand, the best variable to take into account is the mean reach time. This would give us a better idea of the time at which the particles arrive at the detectors, and the results concerning the miniBeBe shine in this field.

In low multiplicities, miniBeBe exhibited superior minimum and mean reach time values compared to FFD. For protons, miniBeBe give us a minimum reach time of 1.53 ns, better 4.657 ns than that obtained by FFD. Similarly, for pions, the miniBeBe achieves a mean reach time of 0.6196 ns respect to 3.516 ns obtained by FFD. Therefore, miniBeBe is notably outperforms FFD in collisions with low multiplicities.

Regarding discrepancies found in Electromagnetic Calorimeter (EMCal) and FFD, several observations can be pointed out. In Section 3.3, we found that the gamma rays resulting from π^0 dacays do exist, with an average of approximately 3.4 gamma rays per event, see Figure 19. And the plausible way to represent these particles is by their conversion to electron-positron pairs in FFD points, where we observed approximately 3 electron-positron pairs.

While there is a tolerable discrepancy between the Monte Carlo simulation and reconstructed data in this case, further analysis is provided. Notably, in the reconstructed data, the number of detected gamma rays is lower, approximately 2 gammas per event, respect to the Monte Carlo Simulations. The discrepancy in the neutral particles detection in EMCal during Monte Carlo simulations, we can suggest that these particles by simulations will disappear in the process of data reconstruction. However, due to time constrains, further investigation in this regard was not possible to perform, and a comprehensive analysis is suggested.

References

[1]C. Alt and et al. (NA49 Collaboration), Phys. Rev. C **79**, 044910 (2009).

[2]T. Anticic and et. al. (NA49 Collaboration), Phys. Rev. C **92**, 044905 (2015).

[3]A. Adare and et. al. (PHENIX Collaboration), Phys. Rev. C **93**, 011901 (2016).

[4]L. Adamczyk and et. al., Physics Letters B **785**, 551–560 (2018).

[5]N. Abgrall and et. al., The European Physical Journal C **79**, 10.1140/epjc/s10052-019-6583-0 (2019).

[6]J. Adam, L. Adamczyk, and et. al. (STAR Collaboration), Phys. Rev. Lett. **126**, 092301 (2021).

[7]V. B. Luong, Moscow University Physics Bulletin **77**, 237–238 (2022).

[8]M. Bleicher, E. Zabrodin, C. Spieles, S. A. Bass, C. Ernst, S. Soff, L. Bravina, M. Belkacem, H. Weber, H. Stöcker, and W. Greiner, Journal of Physics G: Nuclear and Particle Physics **25**, 1859 (1999).

[9]J. Weil and et. al., Phys. Rev. C **94**, 054905 (2016).

[10]Y. Nara, EPJ Web of Conferences **208**, 11004 (2019).

[11]Z.-W. Lin, C. M. Ko, B.-A. Li, B. Zhang, and S. Pal, Phys. Rev. C **72**, 064901 (2005).

[12]A. Taranenko, EPJ Web of Conferences **204**, 03009 (2019).

[13]L. Adamczyk and et. al. (STAR Collaboration), Phys. Rev. C **86**, 054908 (2012).

[14]L. Adamczyk and et. al. (STAR Collaboration), Phys. Rev. C **93**, 014907 (2016).

[15]J. Auvinen and H. Petersen, Phys. Rev. C **88**, 064908 (2013).

[16]I. Karpenko, P. Huovinen, and M. Bleicher, Computer Physics Communications **185**, 10.1016/j.cpc.2014.07.010 (2013).

[17]M. Collaboration, V. Abgaryan, R. Kado, S. Afanasyev, G. Agakishiev, E. Alpatov, G. Altsybeev, M. Hernández, S. Andreeva, T. Andreeva, E. Andronov, N. Anfimov, A. Aparin, V. Astakhov, E. Atkin, T. Aushev, G. Averichev, A. Averyanov, A. Ayala, and D. Zinchenko, 10.48550/arXiv.2202.08970 (2022).

[18]V. I. Yurevich and et al., "Fast forward detector technical design report", MPD TDR (2019).

[19]R. A. Kado et al., "The conceptual design of the miniBeBe detector proposed for NICA-MPD", JINST **16**, P02002 (2021).

[20]MPD/NICA, "Xiii collaboration meeting of the mpd experiment at the nica facility.", (2024).

[21]A. I. M. Golubeva and et al., "Technical design report for the mpd experiment, forward hadron calorimeter", MPD TDR (2018).

[22]A. B. A. Averyanov and et al., "Time projection chamber for multi-purpose detector at nica. technical design report", MPD TDR (2018).